JPEDAV (2009) 30:480–486
DOI: 10.1007/s11669-009-9561-7
1547-7037 ©ASM International

Thermodynamic Assessment of the Cu-B System Supported by Key Experiment and First-Principles Calculations

Wei-Wei Zhang, Yong Du, Honghui Xu, Wei Xiong, Yi Kong, Weihua Sun, Fusheng Pan, and Aitao Tang

(Submitted March 20, 2009)

The Cu-B system was investigated via a hybrid approach of key experiment and thermodynamic modeling. Based on the critically assessed Cu-B phase diagram, seven crucial alloys were selected and prepared by arc melting the pure elements. An inductively coupled plasma-atomic emission spectrometric analysis was conducted to determine the compositions of the prepared alloys. The phase equilibria were determined by using x-ray diffraction, electron probe microanalysis, and differential thermal analysis. The temperature associated with the eutectic reaction, L ⇔ (B) + (Cu), was measured to be 1028 ± 2 °C. First-principles calculations indicate that the energy of inserting a B atom into the interstitial vacancy (Va) site of the lattice for Cu atoms is marginally lower than that of substituting for a Cu atom with a B atom. Consequently, the sublattice model (Cu)(B, Va) in which B atoms occupy the interstitial sites was employed for the fcc (Cu) phase rather than the model (Cu, B)(Va) in which B atoms substitute for Cu atoms. A thermodynamic modeling of the Cu-B system was then performed by considering the reliable literature data and the present experimental results. A good agreement between modeling and experiment was obtained.

Keywords Cu-B, first-principles calculation, phase diagram, thermal analysis, thermodynamic assessment

1. Introduction

B is one of the important metalloids which is added into many transition metal-based materials. B is used in Cu alloys in order to strengthen the grain boundaries[1] and remove harmful impurities at the grain boundaries.[2] It also can be used to deoxidize liquid copper. In addition, the presence of B as a minor element is known to increase the corrosion resistance of Cu alloys.[3] The knowledge of accurate phase equilibria and thermodynamic properties in this binary system is thus of high interest.

This article is an invited paper selected from participants of the 14th National Conference and Multilateral Symposium on Phase Diagrams and Materials Design in honor of Prof. Zhanpeng Jin's 70th birthday, held November 3-5, 2008, in Changsha, China. The conference was organized by the Phase Diagrams Committee of the Chinese Physical Society with Drs. Huashan Liu and Libin Liu as the key organizers. Publication in *Journal of Phase Equilibria and Diffusion* was organized by J.-C. Zhao, The Ohio State University; Yong Du, Central South University; and Qing Chen, Thermo-Calc Software AB.

Wei-Wei Zhang, Yong Du, Honghui Xu, Wei Xiong, Yi Kong, and **Weihua Sun**, State Key Laboratory of Powder Metallurgy, Central South University, Changsha, Hunan 410083, P.R. China; **Wei Xiong**, Department of Materials Science and Engineering, Royal Institute of Technology, SE-100 44 Stockholm, Sweden; **Fusheng Pan** and **Aitao Tang**, College of Materials Science and Engineering, Chongqing University, 400045 Chongqing, P.R. China. Contact e-mail: yongduyong@gmail.com. URL: http://www.imdpm.net.

The Cu-B phase diagram has been experimentally investigated by several groups of authors.[4-7] The major purpose of the present work was to provide an optimal set of thermodynamic parameters for the Cu-B system by means of the CALPHAD approach supplemented with key experiment and first-principles calculation.

2. Review of the Phase Diagram and Thermodynamic Data in the Literature

The available literature data, including phase diagram and thermodynamic data, were critically reviewed in the present work. Table 1 presents the experimental data available in the literature.

2.1 Phase Diagram Data

The first experimental contribution to this system was from Lihl and Feischl[4] using thermal analysis (TA), electronic conductivity analysis, and metallographic analysis. This system was determined to be a eutectic type. The eutectic point is at 10.7 at.% (2.0 wt.%) B and at 1060 ± 2 °C. It was found that the solubility of B in (Cu) is only about 0.35 at.% (0.06 wt.%) at room temperature and rises to 0.53 at.% (0.09 wt.%) at the eutectic temperature. In the work of Smiryagin and Kvurt,[5] TA, metallography, microhardness, and electrical resistivity measurements showed that the system is of the eutectic type with limited solid solubility of B in (Cu). The eutectic point is reported to be at 1021 °C and 10.7 at.% (2 wt.%) B. The solid solubility of B in Cu is about 0.29 at.% (0.05 wt.%) at the eutectic temperature, decreasing to be about 0.06 at.% (0.01 wt.%) at

Table 1 Summary of the phase diagram and thermodynamic data in the Cu-B system

Type of data	Reference	Method	Quoted mode
Liquidus and eutectic point	[4]	TA	•
	[6]	TA	□
	[7]	TA	■
	This work	DTA	■
Solubility of Cu in (B)	This work (1000 °C)	EPMA	■
	[7]	Chemical analysis	■
Solubility of B in (Cu)	[4]	Electronic conductivity measurement	•
	[5]	Electronic resistivity measurements	■
Partial and integral enthalpy of mixing of liquid	[13]	High-temperature solution calorimetry	■
	[14]	High-temperature calorimetry	•
Activity of Cu in liquid	[14]	High-temperature calorimetry	•
Activity of B in liquid	[15]	emf	□
	[3]	Four-phase equilibrium technique	■

TA = thermal analysis; DTA = differential thermal analysis; EPMA = electron probe microanalysis; emf = electromotive force

■: Used in the thermodynamic optimization; □: not used in the thermodynamic optimization, but used to check the final thermodynamic modeling; •: not used in the thermodynamic optimization

room temperature.[5] X-ray diffraction (XRD), metallography, and TA were employed by Wald and Stormont[6] during their investigation of seven Cu-B alloys within a composition range of 1 to 90 at.% B. The eutectic temperature was found to be 1008 °C with the eutectic composition being higher than 10 at.% B. In the work of Rexer and Petzow,[7] six alloys were prepared to determine the liquidus line. Using optical microscopy, XRD, chemical analysis and TA, they[7] determined the eutectic point to be at 13.3 at.% B and 1013 °C. And the maximum solubility of Cu in B is to be 2.8 at.% at 950 °C. The eutectic temperatures reported by three groups of authors[5-7] are lower than that reported by Lihl and Feischl.[4]

Phase diagram data in the Cu-B system have been reviewed by Chakrabarti and Laughlin.[8] The equilibrium phases in this system are liquid, (Cu), and (B). Lihl and Feischl[4] reported that there exists an intermetallic compound CuB_{22} on the B-rich side. However, Smiryagin and Kvurt,[5] Wald and Stormont,[6] and Rexer and Petzow[7] could not confirm the existence of this compound. Based on a thermodynamic calculation, Rao and Anderson[9] examined the phase diagram published in Hansen's *Constitution of Binary Alloys*,[10] and proposed an updated liquidus curve on the Cu-rich side. They[9] stated that CuB_{22} phase is unlikely to exist. Using single-crystal diffractometry, Andersson and Callmer[11] determined the structure of single crystal CuB_{28} which was found to be the β-rhombohedral boron single phase. Higashi et al.[12] synthesized a single crystal of CuB_{23} and determined its crystal structure to be rhombohedral with the lattice parameters of a = 1.0985 nm and c = 2.3925 nm. According to the work of Higashi et al.,[12] the structure of this crystal is identical to β-rhombohedral B.

2.2 Thermodynamic Data

Limited thermodynamic data at Cu-rich side are available for this system. Using high-temperature solution calorimetry, Kleppa and Sato[13] measured the enthalpies of mixing relative to solid B and liquid Cu at 1108 °C in the range 0-10.5 at.% B. Batalin et al.[14] measured the partial and integral enthalpies of mixing of liquid and activities of the B in liquid phase on the Cu-rich side at 1517 °C by means of high-temperature calorimetry. Using electromotive force (emf) measurements, Yukinobu et al.[15] measured the activities of B in the Cu-B melts with 2 and 4 at.% B at 1150, 1200 and 1250 °C. Employing a four-phase equilibrium technique, which can be considered as an extension of the conventional procedure involving metal-slag-gas equilibration, Jacob et al.[3] reinvestigated the activity of B in liquid phase at 1450 °C. The data of Jacob et al.[3] and Kleppa and Sato[13] were included in the thermodynamic optimization.

3. Experimental Procedures

In order to check the general feature of the Cu-B phase diagram and provide new phase diagram data for the thermodynamic optimization, seven key samples were prepared with starting materials of 99.99 wt.% Cu and 99.95 wt.% B. Compositions of the prepared alloys are shown in Table 2. The alloys were prepared with an arc melter (WKDHLI, Beijing Opto-electronics Co. Ltd., China) on a water-cooled copper plate under an argon atmosphere. Each alloy was remelted three times to ensure homogeneity. The mass losses during arc-melting were large since B particles were splitting during arc-melting. Each sample was thus cut into several parts. One part was used for the inductively coupled plasma-atomic emission spectrometry (ICP-AES, ADVANTAGE-1000, TJA) measurements in order to obtain an accurate alloy composition. Portions of the second part were wrapped with Mo filaments, sealed in evacuated quartz capsules, and then annealed at two different temperatures (1000 °C for 265 h

Table 2 Summary of the alloy composition, the identified phases and the phase transition temperatures in the Cu-B system

	Nominal comp. (B%)		Measured comp. (B%) (a)					
No.	at.%	wt.%	at.%	wt.%	Temperature, °C	Phase	Composition (at.% B)	DTA signal, °C
1	10	1.85	5.18	0.92	850	(Cu)		↑1029.1 (onset), 1074.0 (peak)
						(B)		↓1051.2 (onset)
2	13	2.48	7.96	1.45	850	(Cu)		↑1030.9 (onset), 1069.7 (peak)
						(B)		↓999.0 (peak), 1040.5 (onset)
3	15	2.91	9.83	1.82	850	(Cu)		↑1029.6 (onset), 1053.7 (inflection)
						(B)		↓1000.6 (peak), 1027.6 (onset)
4	25	5.36	17.57	3.50	850	(Cu)		↑1026.1 (onset)
						(B)		↓985.5 (peak), 1132.1 (onset)
5	35	8.39	…	…	1000	(Cu)	…	…
						(B)	96.59	…
6	45	12.22	34.4	8.19	850	(Cu)		↑1026.2 (onset)
						(B)		↓998.4 (peak)
7	50	14.54	38.93	10.54	850	(Cu)		↑1026.3 (onset)
						(B)		↓993.9 (peak), 1450.0 (onset)

(a) Measured with ICP-AES method

↑ means the thermal effects on the heating curve and ↓ means the thermal effects on the cooling curve

and 850 °C for 500 h) to achieve homogeneity. The third part in its as-cast state was used to observe the microstructure associated with the invariant reaction.

After quenching by rapidly submersing the capsules in water, the samples were investigated by means of XRD, optical microscopy, electron probe microanalysis (EPMA) and differential thermal analysis (DTA). The phase identification was performed by means of XRD (Rigaku D-max/2550 VB^{+}, Japan) at 40 kV and 300 mA with Cu-Kα radiation. Microstructure of the solidified and annealed alloys was observed by optical microscopy (Leica DMLP, Wetzlar GmbH, Germany). Phase compositions of some equilibrated alloys were obtained via EPMA (JXA-8800R, JEOL, Japan) method.

DTA (DSC404C, NETZSCH, Germany) was used to measure phase transition temperatures. The measurements were performed in an argon atmosphere between room temperature and 1450 °C with the heating and cooling rate of 5 °C/min. This DTA apparatus was calibrated to the melting points of Al (660.32 °C), Au (1064.18 °C), and Si (1413.85 °C). In the temperature range examined, the accuracy of the temperature measurements was estimated to be ±2 °C. The invariant reaction temperature was determined from the onset of the first thermal effect during the heating step, and the peak temperature of the second thermal effect on heating was taken for the liquidus.

4. First-Principles Calculations

Due to the peculiar interplay of atomic size, B could be in the interstitial position or in the substitutional position for Cu lattice. In the present work, first-principles calculations were employed to decide whether the interstitial model or the substitutional model was valid for (Cu) phase. Vienna ab initio simulation package (VASP)[16] was utilized for the calculation. Fully relaxed geometry optimization was performed to find the ground state of the studied structures. The calculations were conducted in a plane-wave basis with maximum cut-off energy of 400 eV, using Project-Augment-Wave potential[17] to describe the electron-ion interaction, and the pseudo atomic calculations performed for Cu and B are $3p^{6}3d^{10}4s^{1}$ and $2s^{2}2p^{1}$, respectively. The exchange and correlation items are described by the generalized-gradient approximation (GGA).[18] The integration in the Brillouin zone (BZ) is done on the special *k* points determined from the Monkhorst-Pack scheme.[19]

Two supercells for the two different occupation patterns of the B atom into the lattice of the Cu atoms are constructed. The supercell for interstitial occupation has 49 atoms, in which 48 Cu atoms occupy the perfect fcc lattice, while one B atom occupies the central octahedral interstitial site. The other supercell for substitutional occupation has 32 atoms, in which 31 Cu atoms occupy the perfect fcc lattice, while a B atom substitutes for a Cu atom in the central site of the perfect fcc lattice.

The present first-principles calculations show that the energy of inserting a B atom into the interstitial site of the lattice for Cu caused the energy of the supercell system to rise by 1.858 eV, which is lower than that of the substitutional occupation with the value of 1.901 eV. The result suggests that the interstitial occupation mechanism is marginally more stable than the substitutional occupation one. Consequently, the model $(Cu)_1(B, Va)_1$ was selected for the (Cu) phase.

5. Thermodynamic Modeling

Based on the experimental data from the literature and present work, a thorough thermodynamic optimization of the Cu-B system was then conducted. The thermodynamic properties of Cu and B are taken from the SGTE compilation.[20] The Gibbs energy of the liquid is described by the Redlich-Kister polynomials[21]:

$$\begin{aligned} G_m^L - H^{\mathrm{SER}} &= (1-x_{\mathrm{B}})\cdot {}^0G_{\mathrm{Cu}}^L + x_{\mathrm{B}}\,{}^0G_{\mathrm{B}}^L \\ &+ RT[x_{\mathrm{B}}\ln x_{\mathrm{B}} + (1-x_{\mathrm{B}})\ln(1-x_{\mathrm{B}})] \\ &+ x_{\mathrm{B}}(1-x_{\mathrm{B}})[a_0 + b_0T + c_0T\ln(T) \\ &+ (1-2x_{\mathrm{B}})(a_1 + b_1T + c_1T\ln(T)) + \cdots] \end{aligned} \quad \text{(Eq 1)}$$

in which H^{SER} is the abbreviation of $(1-x_{\mathrm{B}})H_{\mathrm{Cu}}^{\mathrm{SER}} + x_{\mathrm{B}}H_{\mathrm{B}}^{\mathrm{SER}}$, R is the gas constant, and x_{B} is the mole fraction of B. The interaction parameters a_0, b_0, c_0, a_1, b_1 and c_1 could be optimized from the experimental phase diagram and thermodynamic data.

The present first-principles calculation has demonstrated that the model $(\mathrm{Cu})_1(\mathrm{B,Va})_1$ can be used to describe (Cu). According to the sublattice model,[22] the Gibbs energy for (Cu) is represented by the following equation:

$$\begin{aligned} &G_{\mathrm{Cu:B,Va}}^{\mathrm{fcc\_A1}} - H^{\mathrm{SER}} \\ &= y''_{\mathrm{B}}G_{\mathrm{Cu:B}}^{\mathrm{fcc\_A1}} + y''_{\mathrm{Va}}G_{\mathrm{Cu:Va}}^{\mathrm{fcc\_A1}} + RT\left(y''_{\mathrm{B}}\ln y''_{\mathrm{B}} + y''_{\mathrm{Va}}\ln y''_{\mathrm{Va}}\right) \\ &+ y''_{\mathrm{B}}y''_{\mathrm{Va}}\left(\sum_{j=0,1\ldots} {}^{(j)}L_{\mathrm{Cu:B,Va}}^{\mathrm{fcc\_A!}}\left(y''_{\mathrm{B}} - y''_{\mathrm{Va}}\right)^j\right) \end{aligned} \quad \text{(Eq 2)}$$

$$G_{\mathrm{Cu:B}}^{\mathrm{fcc\_A1}} = {}^0G_{\mathrm{Cu}}^{\mathrm{fcc\_A1}} + {}^0G_{\mathrm{B}}^{\mathrm{fcc\_A1}} \quad \text{(Eq 3)}$$

$${}^{(j)}L_{\mathrm{Cu:B,Va}}^{\mathrm{fcc\_A1}} = A_j + B_jT + C_jT\ln(T) \quad \text{(Eq 4)}$$

where y''_{B} and y''_{Va} are the site fractions of B and vacancy in the second sublattice, respectively.

Based on the crystal structure of B,[23] (B) is modeled with a two-sublattice $(\mathrm{B})_{93}(\mathrm{B,Cu})_{12}$. This two-sublattice model has been used to describe (B) in the B-Zr system in the form of sublattice $(\mathrm{B})_{93}(\mathrm{B,Zr})_{12}$[24] and (B) in the C-Si-B system with the sublattice $(\mathrm{B})_{93}(\mathrm{B,C,Si})_{12}$. Thus, a model $(\mathrm{B})_{93}(\mathrm{B,X,Y,Z})_{12}$ is recommended to describe (B) phase in multi-component systems. The Gibbs energy of (B) in the Cu-B system is thus formulated as:

$$\begin{aligned} G_m^{\beta-\mathrm{B}} - H^{\mathrm{SER}} &= y''_{\mathrm{B}}\cdot {}^0G_{\mathrm{B:B}}^{\beta-\mathrm{B}} + y''_{\mathrm{Cu}}G_{\mathrm{B:Cu}}^{\beta-\mathrm{B}} \\ &+ 12RT\left(y''_{\mathrm{B}}\ln y''_{\mathrm{B}} + y''_{\mathrm{Cu}}\ln y''_{\mathrm{Cu}}\right) \\ &+ y''_{\mathrm{B}}y''_{\mathrm{Cu}}\left(\sum_{j=0,1\ldots} {}^{(j)}L_{\mathrm{B:B,Cu}}^{\beta-\mathrm{B}}\left(y''_{\mathrm{B}} - y''_{\mathrm{Cu}}\right)^j\right) \end{aligned} \quad \text{(Eq 5)}$$

$$G_{\mathrm{B:B}}^{\beta-\mathrm{B}} = 105\,{}^0G_{\mathrm{B}}^{\beta-\mathrm{B}}$$

$$G_{\mathrm{B:Cu}}^{\beta-\mathrm{B}} = 12\,{}^0G_{\mathrm{Cu}}^{\mathrm{fcc\_Cu}} + 93\,{}^0G_{\mathrm{B}}^{\beta-\mathrm{B}} + A + BT \quad \text{(Eq 6)}$$

$${}^{(j)}L_{\mathrm{B:B,Cu}}^{\beta-\mathrm{B}} = A_j + B_jT \quad \text{(Eq 7)}$$

in which y''_{B} and y''_{Cu} are the site fractions of B and Cu in the second sublattice, respectively.

6. Results and Discussion

Table 2 summarizes the compositions of the alloys determined with ICP-AES method, phases identified with XRD and the phase transition temperatures resulting from DTA measurements. In these measurements which are found to be consistently reproducible, XRD examinations of the samples in both annealed and as-cast states show the existence of (Cu) and (B). The nominal composition of the alloy against the one measured with ICP-AES is presented in Fig. 1, showing a linear relationship between them. The significance of this figure is that one can derive the actual composition of the prepared alloy from its nominal composition.

DTA measurements on the alloys provide new phase transition temperatures. The presently measured eutectic temperature of the $\mathrm{L} \Leftrightarrow (\mathrm{B}) + (\mathrm{Cu})$, is at 1028 ± 2 °C, which is close to that in Ref 5 but is higher by 15 °C than that reported in Ref 7.

Figure 2 shows the backscattered electron (BSE) image of alloy 5 equilibrated at 1000 °C, clearly showing the coexistence of (B) and (Cu). The solubility of Cu in (B) was determined to be 3.4 at.% Cu at 1000 °C which is consistent with the work of Rexer and Petzow[7] and Higashi et al.[12]

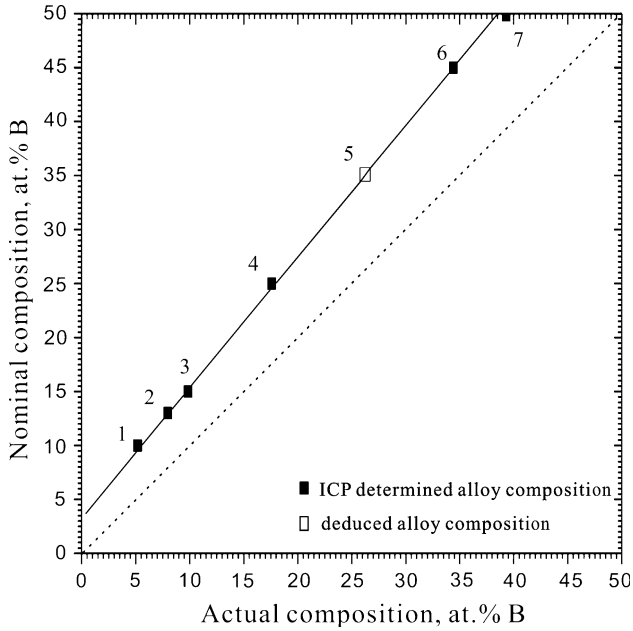

Fig. 1 Nominal and actual compositions of the prepared Cu-B alloys. From the linear relationship, the actual composition of alloy 5 with nominal composition of 35 at.% B is deduced to be 26.3 at.% B

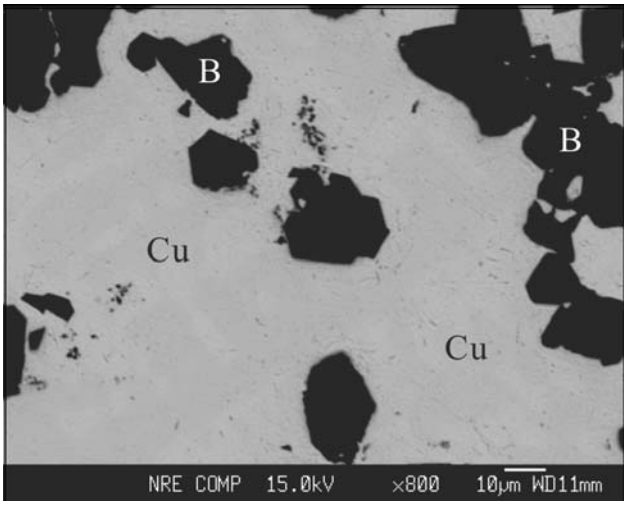

Fig. 2 Back scattering electron micrograph of alloy 5 (nominal composition 35 at.% B) annealed at 1000 °C for 14 days

Table 3 Presently optimized thermodynamic parameters in the B-Cu system (J/mole-atoms)

Phase	Thermodynamic parameters
Liquid: (B,Cu)	${}^{0}L_{B,Cu} = -264.2$
	${}^{1}L_{B,Cu} = 9050.1$
	${}^{2}L_{B,Cu} = 24616.6$
(Cu): (Cu)(B, Va)	${}^{0}L^{fcc}_{Cu:B,Va} = 33007.7$
(B): $(B)_{93}(B,Cu)_{12}$	$G^{\beta-B}_{B:Cu} = 12\,{}^{0}G^{fcc\_Cu}_{Cu} + 93\,{}^{0}G^{\beta-B}_{B} + 117316$

The currently obtained experiment data plus the data of Rexer and Petzow[7] are utilized in the thermodynamic optimization.

The evaluation of the model parameters is attained by recurrent runs of the PARROT program,[25] which works by minimizing the square sum of the differences between experimental values and computed ones. In the optimization, each piece of experimental information is given a certain weight. The weights were changed systematically during the assessment until most of the experimental data were accounted for within the claimed uncertainty limits.

The optimization began with the liquid phase. For liquid, according to the analytical expression which describes the experimental enthalpies of mixing,[13] three coefficients a_0, a_1, a_2 were used in the optimization. Secondly, the (B) phase was considered in the optimization. It was found that one parameter can describe the liquidus at (B)-rich side and B solubility well. Thirdly, the parameters of fcc (Cu) are added to optimize the experiment data of the (Cu)-rich side. At last all experimental data were used in the global optimization. The thermodynamic parameters obtained in the present work are listed in Table 3.

Figure 3(a) presents the calculated Cu-B phase diagram using the presently evaluated thermodynamic parameters,

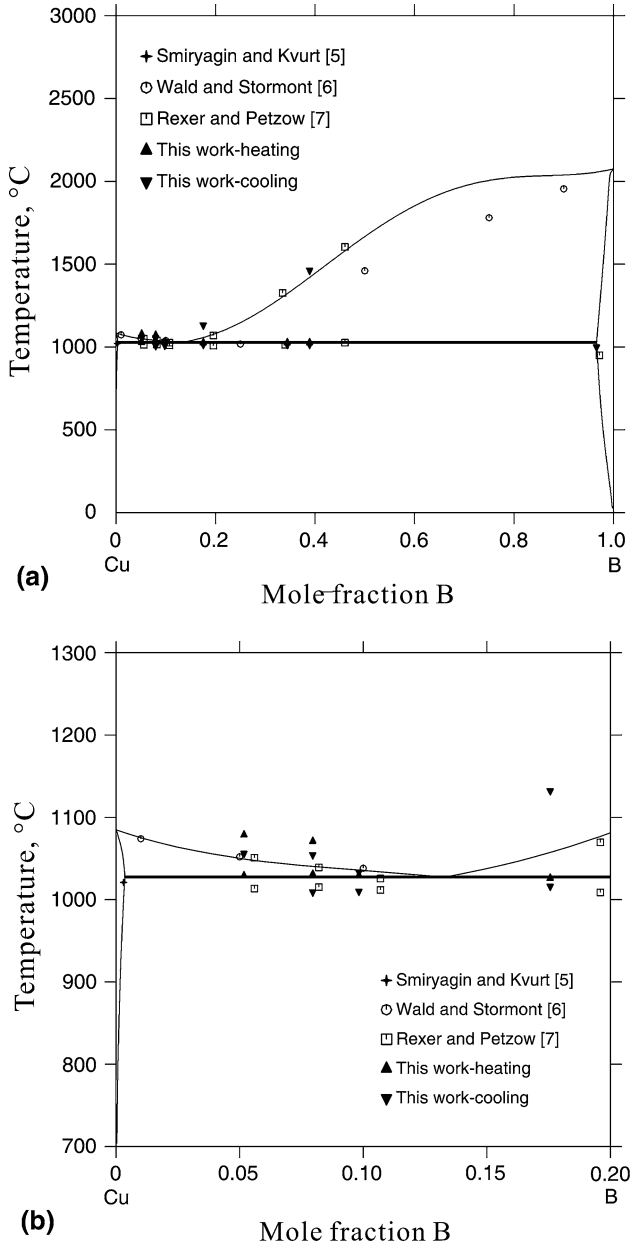

Fig. 3 (a) Calculated Cu-B phase diagram, compared with the experimental data from the present work and the literature[5-7]; (b) close up on the phase equilibria in Cu-rich corner

compared with the present experimental results and the reliable literature data,[4-7] showing that the calculated result is in good agreement with the experimental data. The calculated eutectic point is at 1027 °C and 13.3% B. And the solubilities of (Cu) and (B) phases at 1027 °C are 0.36 at.% B and 96.6 at.% B, respectively. The presently computed phase diagram was confirmed to be a stable one with the Pandat[26] programs. An enlarged Cu-rich region showing the detail of the equilibrium is presented in Fig. 3(b).

Figure 4 presents the calculated enthalpy of mixing of liquid phase at 1108 °C with liquid Cu and solid B being

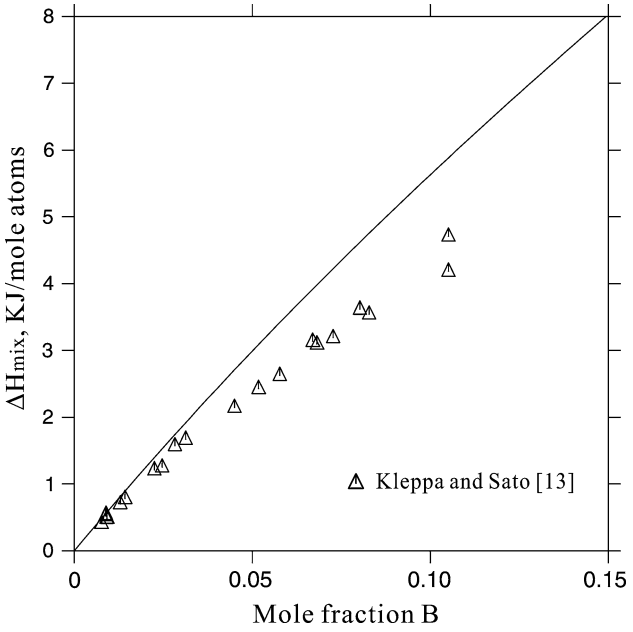

Fig. 4 Comparison between the calculated and measured enthalpy of mixing of liquid phase at 1108 °C, and the reference state are liquid Cu and solid B

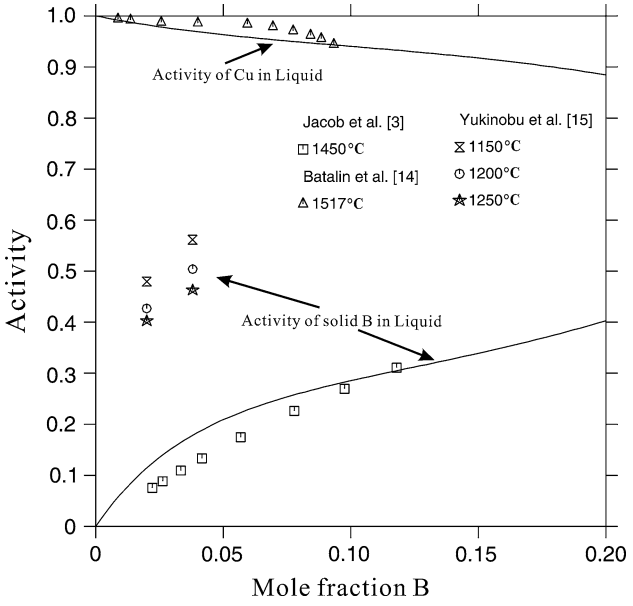

Fig. 5 Comparison between the calculated and measured activities[3,14,15] of B and Cu in liquid at 1450 °C. The reference state is solid B and liquid Cu

reference state. The agreement with the experimental data of Kleppa and Sato[13] is good.

Figure 5 shows the calculated activities of B and Cu in liquid phase at 1450 °C versus the experimental data from Jacob et al.[3] The experimental data of Batalin et al.[14] and Yukinobu et al.,[15] which were not used in the optimization, were also plotted in Fig. 5. The original activity data[14,15] are converted to the temperature of 1450 °C via the function, $a^{\exp}(T_{\exp}) + a^{\text{cal}}(1450\,^{\circ}\text{C}) - a^{\text{cal}}(T_{\exp})$, where $T_{\exp}$ is the experimental temperature, $a^{\exp}(T_{\exp})$ is the measured activity value at the experimental temperature, $a^{\text{cal}}(1450\,^{\circ}\text{C})$ and $a^{\text{cal}}(T_{\exp})$ are the calculated ones at 1450 °C and experimental temperature, respectively. The reference state is solid boron and liquid copper. The present calculation shows a reasonable agreement with the experimental value.[3,14] The experimental values from Yukinobu et al.[15] are found to be unreliable.

7. Conclusions

The phase equilibria in the Cu-B system were reinvestigated using seven decisive alloys subjected to XRD, DTA and ICP-AES measurements. The presently obtained phase equilibria were incorporated into the modeling, yielding an accurate thermodynamic description of the Cu-B system. First-principles calculations were employed to choose an appropriate thermodynamic model for (Cu) phase.

A thermodynamic modeling of the Cu-B system was carried out by using the experimental data in the literature and those from the present work. A self-consistent set of thermodynamic parameters was obtained.

Acknowledgments

The financial support from the Creative Research Group of National Natural Science Foundation of China (Grant No. 50721003) and the National Outstanding Youth Science Foundation of China (Grant No. 50425103) are acknowledged. The Thermo-Calc Software AB in Sweden is gratefully acknowledged for the provision of Thermo-Calc software. Thanks are also due to Alexander Von Humboldt foundation of Germany for the donation of Leica DMLP optical microscopy.

References

1. A.Y. Lozovoi and A.T. Paxton, Boron in Copper: A Perfect Misfit in the Bulk and Cohesion Enhancer at a Grain Boundary, *Phys. Rev. B*, 2008, **77**(16), p 165413
2. R. Suryanarayanan, C.A. Frey, S.M.L. Sastry, B.E. Waller, S.E. Bates, and W.E. Buhro, Plastic Deformation of Nanocrystalline Cu and Cu-0.2 wt.% B, *Mater. Sci. Eng. A*, 1999, **264**, p 210-214
3. K.T. Jacob, S. Priya, and Y. Waseda, Measurement of the Activity of Boron in Liquid Copper Using a Four-Phase Equilibrium Technique, *Metall. Mater. Trans. A*, 2000, **31A**, p 2674-2678
4. F. Lihl and O. Feischl, Preparation and Constitution of Copper-Boron Alloys, *Metall*, 1954, **8**, p 11-19, in German
5. A.P. Smiryagin and O.S. Kvurt, The Copper-Boron Constitutional Diagram, *Tr. Nauchn. IssIed Proektn. Inst. Splavov Obrabot. Tsvet. Metal.*, 1965, **24**, p 7-11, in Russian (Chem. Abstr. 64:13863h)
6. F. Wald and R.W. Stormont, Investigations on the Constitution of Certain Binary Boron-Metal Systems, *J. Less-Common Met.*, 1965, **9**, p 423-433

7. J. Rexer and G. Petzow, About the Buildup and Some Properties of Cu-B Alloys, *Metallurgy*, 1970, **24**, p 1083-1086, in German
8. D.J. Chakrabarti and D.E. Laughlin, The B-Cu (Boron-Copper) System, *Bull. Alloy Phase Diagram*, 1982, **3**, p 45-48
9. M.V. Rao and R.N. Anderson, Reassessment of the Copper-Boron Phase Diagram, *J. Less-Common Met.*, 1971, **25**, p 427-430
10. M. Hansen and K. Anderko, *Constitution of Binary Alloys*, 2nd ed., McGraw-Hill, New York, 1958, p 248-249
11. S. Andersson and B. Callmer, The Solubilities of Copper and Manganese in β-Rhombohedral Boron as Determined in CuB_{28} and MnB_{23} by Single Crystal Diffractometry, *J. Solid State Chem.*, 1974, **10**, p 219-231
12. I. Higashi, T. Sakurai, and T. Atoda, Crystal Structure of CuB_{23}, *J. Less-Common Met.*, 1976, **45**, p 283-292
13. O.J. Kleppa and S. Sato, New Application of High-Temperature Solution Calorimetry III. Enthalpies of Formation of Mn_2B, MnB, and MnB_2, *J. Chem. Thermodynamics*, 1982, **14**, p 133-143
14. G.I. Batalin, V.S. Sudavtsova, and M.V. Mikhaiolvskaya, Thermodynamic Properties of Molten Copper-Boron Alloys, *Izvest. Vyssh. Ucheb. Zaved. Tsvetn. Metall.*, 1985, **2**, p 125-127
15. M. Yukinobu, O. Ogawa, and S. Goto, Activities of Boron in the Binary Iron-Boron, Cobalt-Boron, and Copper Boron Melts, *Metall. Trans. B*, 1989, **28B**, p 705-710
16. G. Kresse and J. Furthmüller, Efficiency of Ab Initio Total Energy Calculations for Metals and Semiconductors Using a Plane-Wave Basis Set, *Comput. Mater. Sci*, 1996, **6**, p 15-50
17. G. Kresse and D. Joubert, From Ultrasoft Pseudopotentials to the Projector Augmented-Wave Method, *Phys. Rev. B*, 1999, **59**, p 1758-1775
18. J.P. Perdew and Y. Wang, Accurate and Simple Analytic Representation of the Electron-Gas Correlation Energy, *Phys. Rev. B*, 1992, **45**, p 13244-13249
19. H.J. Monkhorst and J.D. Pack, Special Points for Brillouin-Zone Integrations, *Phys. Rev. B*, 1976, **13**, p 5188-5192
20. A.T. Dinsdale, SGTE Data for Pure Elements, *CALPHAD*, 1991, **15**, p 317-425
21. O. Redlich and A.T. Kister, Thermodynamics of Nonelectrolyte Solutions, x-y-t Relations in a Binary System, *Ind. Eng. Chem.*, 1948, **40**, p 345-348
22. M. Hillert and L.-I. Staffansson, Regular Solution Model for Stoichiometric Phases and Ionic Melts, *Acta Chem. Scand.*, 1970, **24**(10), p 3618-3626
23. P. Villars and L.D. Calvert, *Pearson's Handbook of Crystallographic Data for Intermetallic Phases*, 2nd ed., ASM International, Materials Park, OH, 1991
24. H.M. Chen, F. Zheng, H.S. Liu, L.B. Liu, and Z.P. Jin, Thermodynamic Assessment of B-Zr and Si-Zr Binary Systems, *J. Alloys Compd.*, 2009, **468**, p 209-216
25. B. Sundman, B. Jansson, and J.O. Andersson, The Thermo-Calc Databank System, *CALPHAD*, 1985, **9**, p 153-190
26. S.-L. Chen, S. Daniel, F. Zhang, Y.A. Chang, W.A. Oates, and R. Schmid-Fetzer, PanEngine 1.0-Phase Equilibrium Calculation Engine for Multi-Component Systems, Madison, WI, Computherm LLC, 2000